Data Supplement

Aligned nanofibrillar collagen scaffolds – Guiding lymphangiogenesis for treatment of secondary lymphedema

Catarina Hadamitzky, Tatiana S. Zaitseva, Magdalena Bazalova-Carter, Michael V. Paukshto, Luqia Hou, Zachary Strassberg, James Ferguson , Yuka Matsuura , Rajesh Dash , Phillip C. Yang, Shura Kretchetov, Peter M. Vogt, Stanley G. Rockson, John P. Cooke, Ngan F. Huang

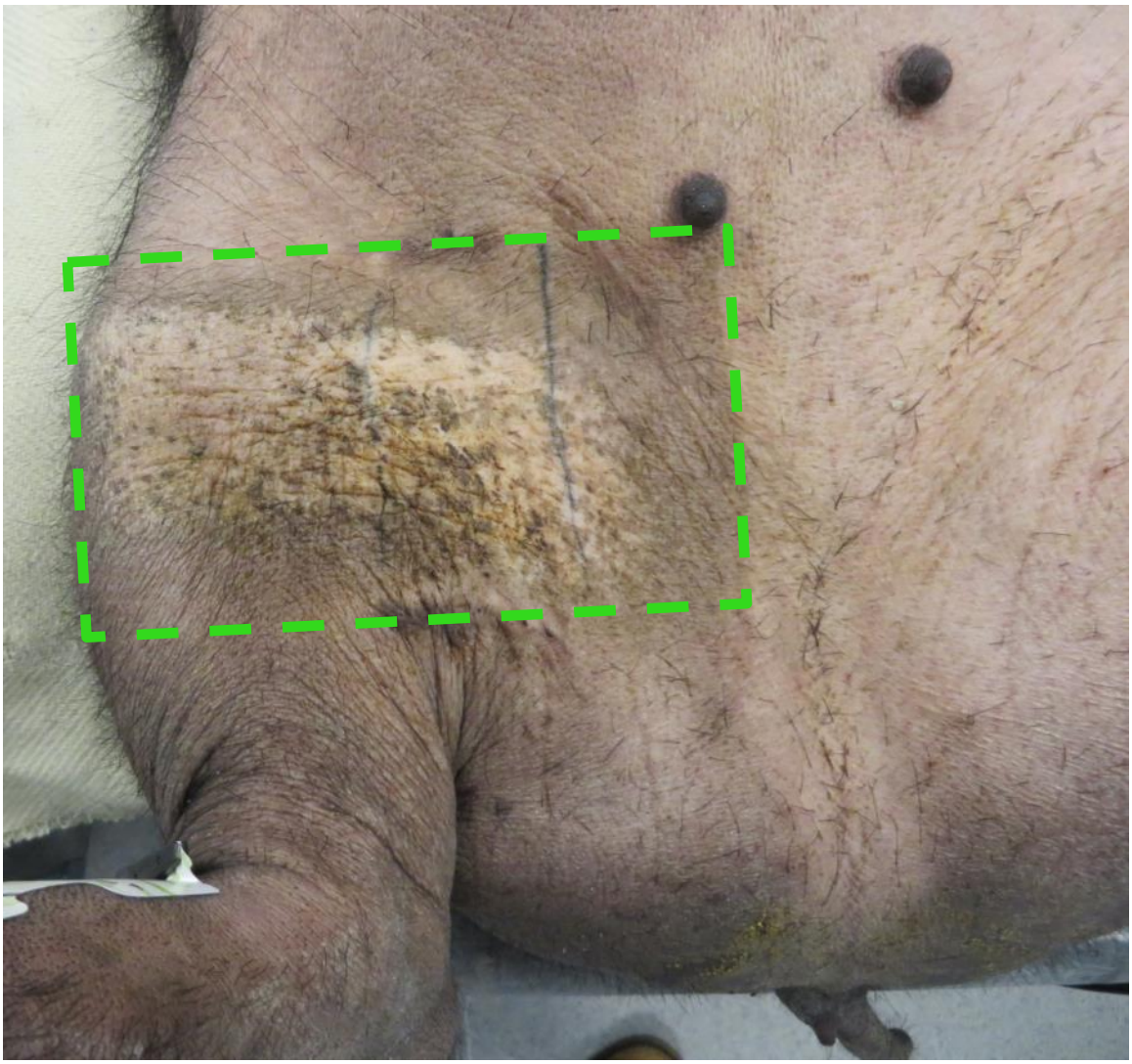

Supplementary Fig. 1. Description of the irradiation area in the minipig model for secondary lymphedema. The green rectangle shows the anatomic area subjected to lymphatic resection and radiation at the time point of 3 months before study start. Note the presence of dermal radio-damage and tissue contraction, very comparable to the changes observed in human patients.

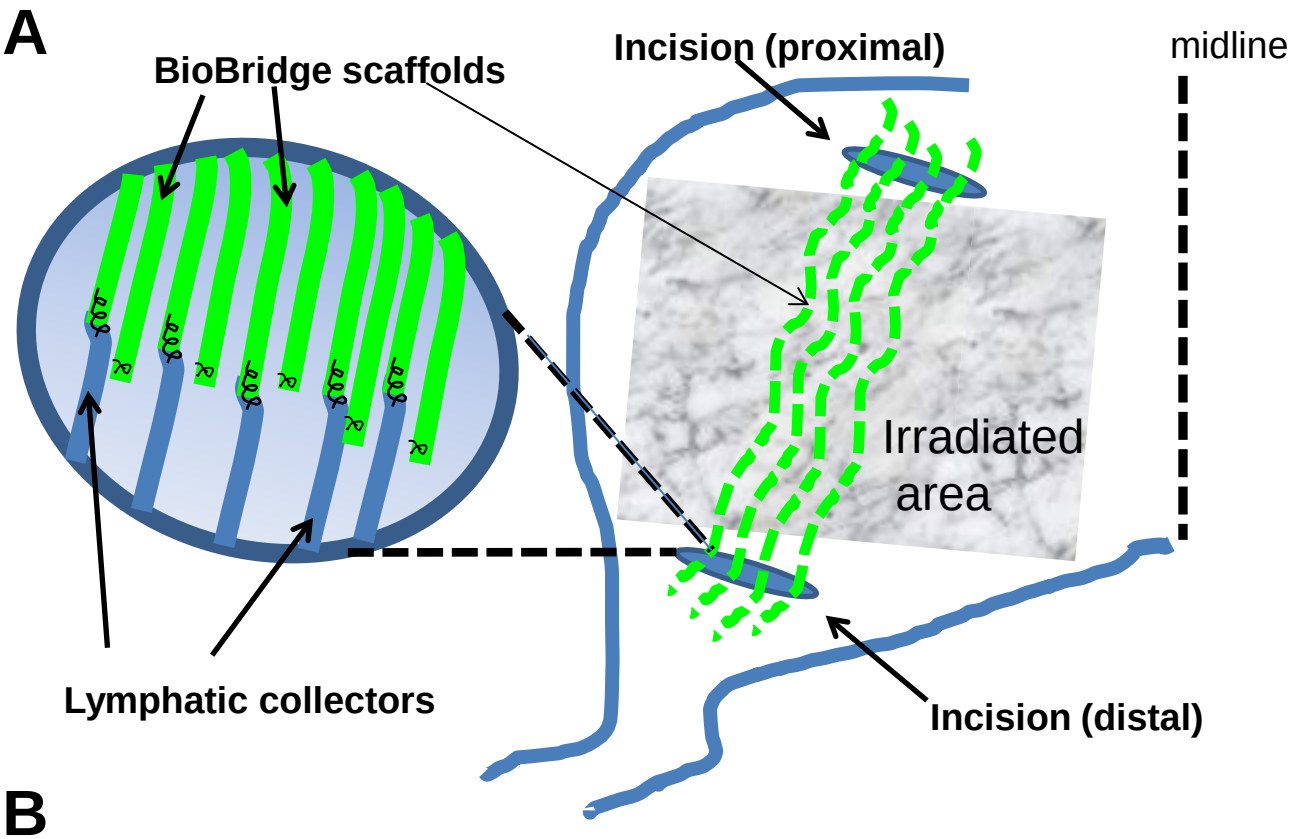
A
BioBridge scaffolds
Incision (proximal)
midline
Irradiated area
Lymphatic collectors
Incision (distal)

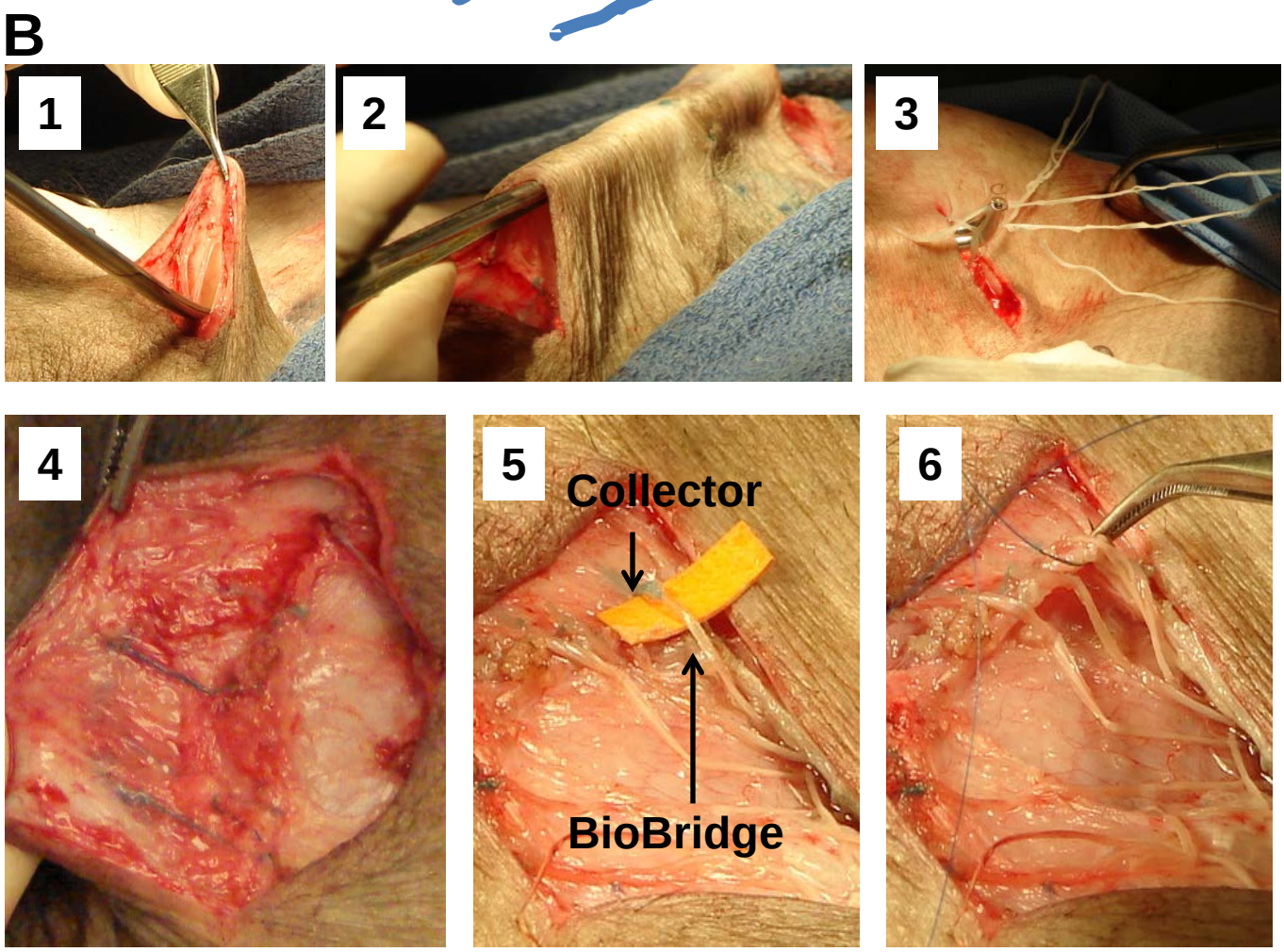
B
1
2
3
4
5
Collector
BioBridge
6

Supplementary Fig. 2. Overview of *in vivo* scaffold implantation procedure. **A.** Schematic overview of surgical implantation procedure. Biobridge scaffolds were implanted to span across the irradiated area with lymphatic collectors removed though two incisions, with half of the scaffolds sutured to the remaining ends of collectors, and the other half sutured to the surrounding tissue. **B.** Detailed scaffold implantation. (1) Proximal and distal incisions were made first. (2) Then, a tunnel was created between the two incisions. (3) The scaffolds were pulled though this tunnel. (4) Next, the remaining collectors were identified. (5) Scaffolds were sutured to the existing lymphatic collectors and (6) to surrounding tissue, according to the schematic shown (A).

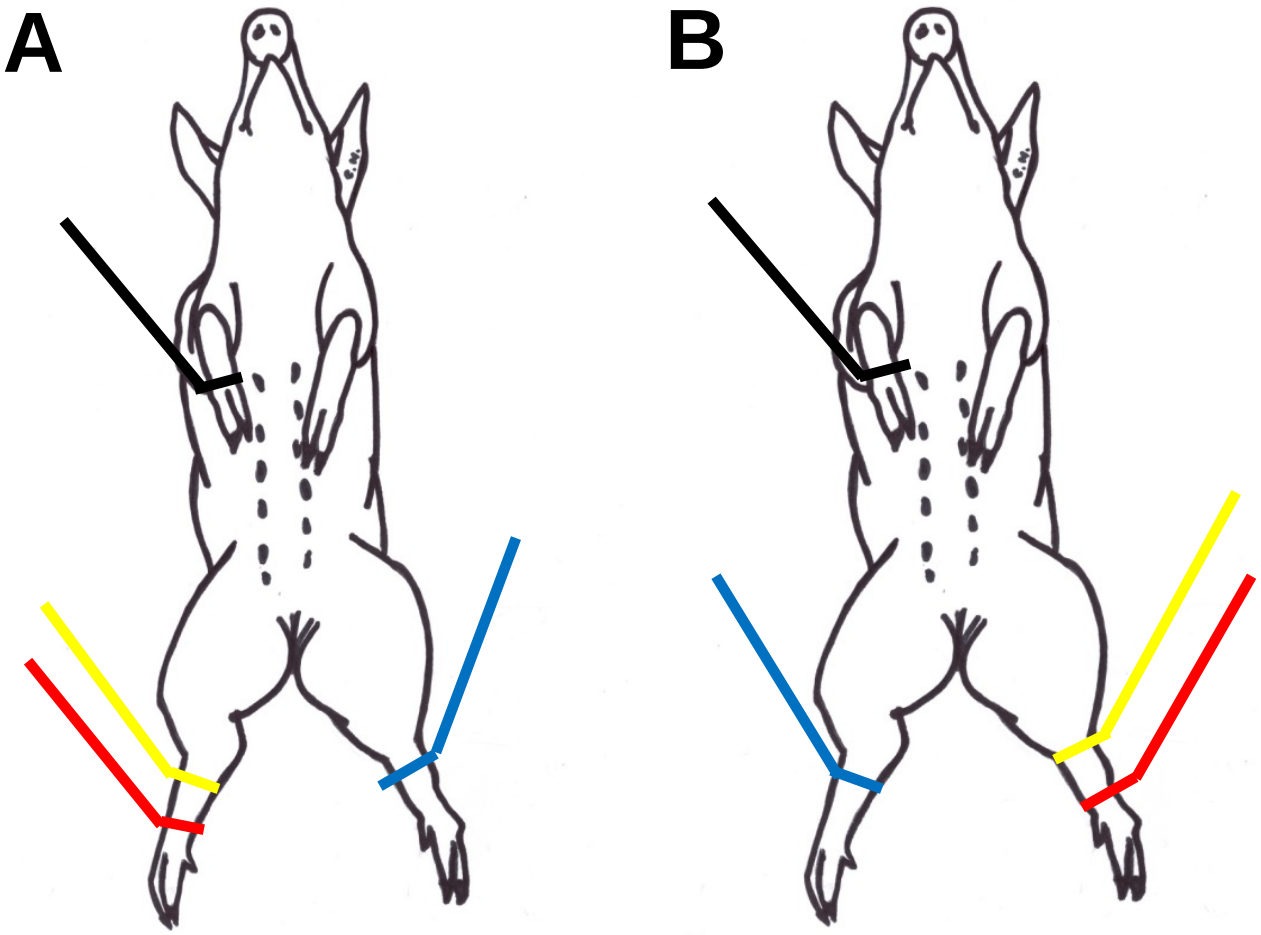

Supplementary Fig. 3. Bioimpedance measurement configuration. A. Positioning of contact electrodes for the measurement of the bioimpedance of the right hind limb. Measurement electrodes are depicted in blue and yellow. Black and red electrodes represent the electric current injection sites. B. Positioning of the same electrodes for the measurement of the bioimpedance of the left hind limb. The measurement table was made of a non-conducting plastic material.

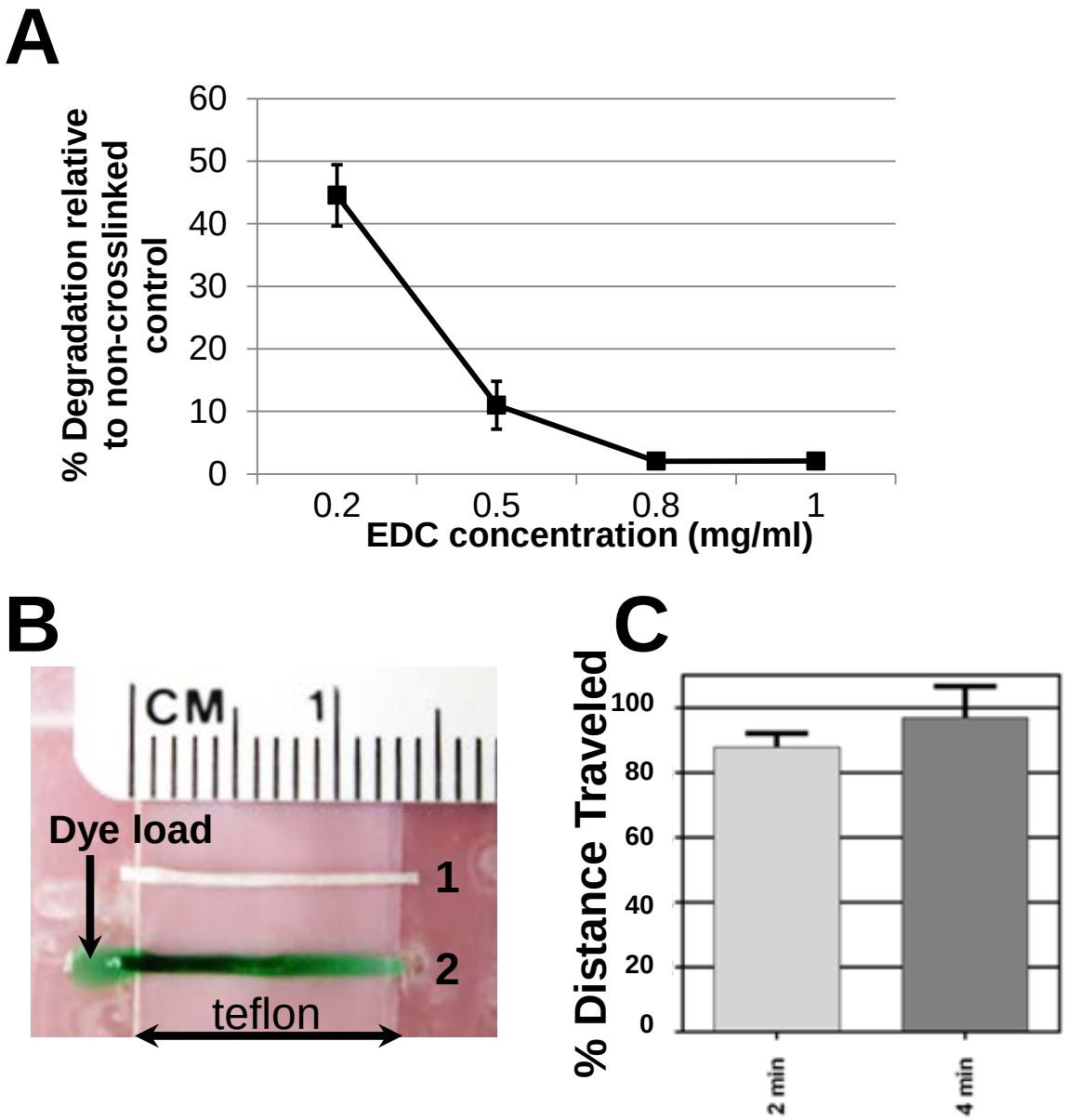

Supplementary Fig. 4. Functional characterization of nanofibrillar collagen scaffolds. A. Relationship between crosslinker (EDC) concentration and BioBridge degradation. Enzymatic degradation was performed by incubation in bacterial collagenase for 4 h, and the degraded collagen in solution was quantified by reacting with 2% ninhydrin. Data were normalized by scaffold mass and expressed as percentage of the degradation of non-crosslinked material (n = 3) **B.** Capillarity measurement setup with scaffold placement on the hydrophobic teflon surface: (1) scaffold sample prior to application of the green dye; (2) scaffold sample at 4 min after the green dye load. A syringe with 25G needle was used to deliver approximately 0.1 mL of green food coloring dye to the left end of BioBridge. **C.** Quantification of the dye travelling distance with respect to the BioBridge length. (n = 20).

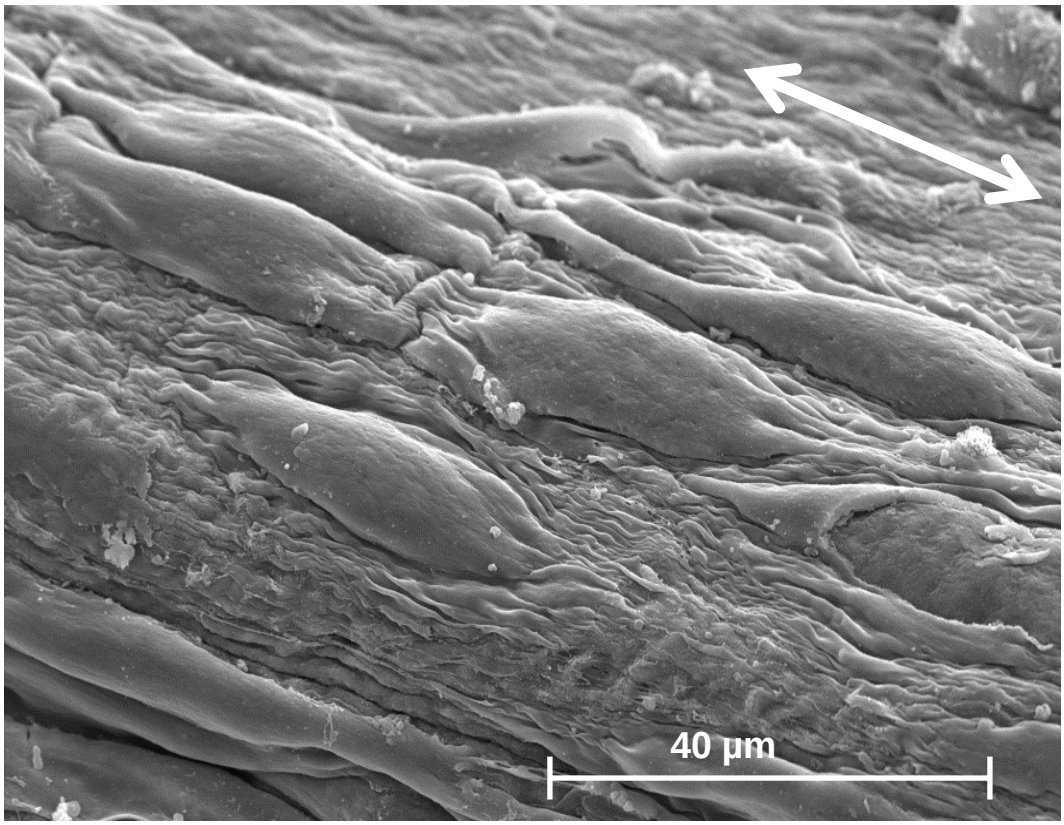

Supplementary Fig. 5. Morphological endothelial cell reorganization along the collagen scaffolds. Scanning electron microscopy imaging of lymphatic endothelial cells assembled on the scaffold in the direction of collagen nanofibrils (arrow). Scale bar, 40 µm.

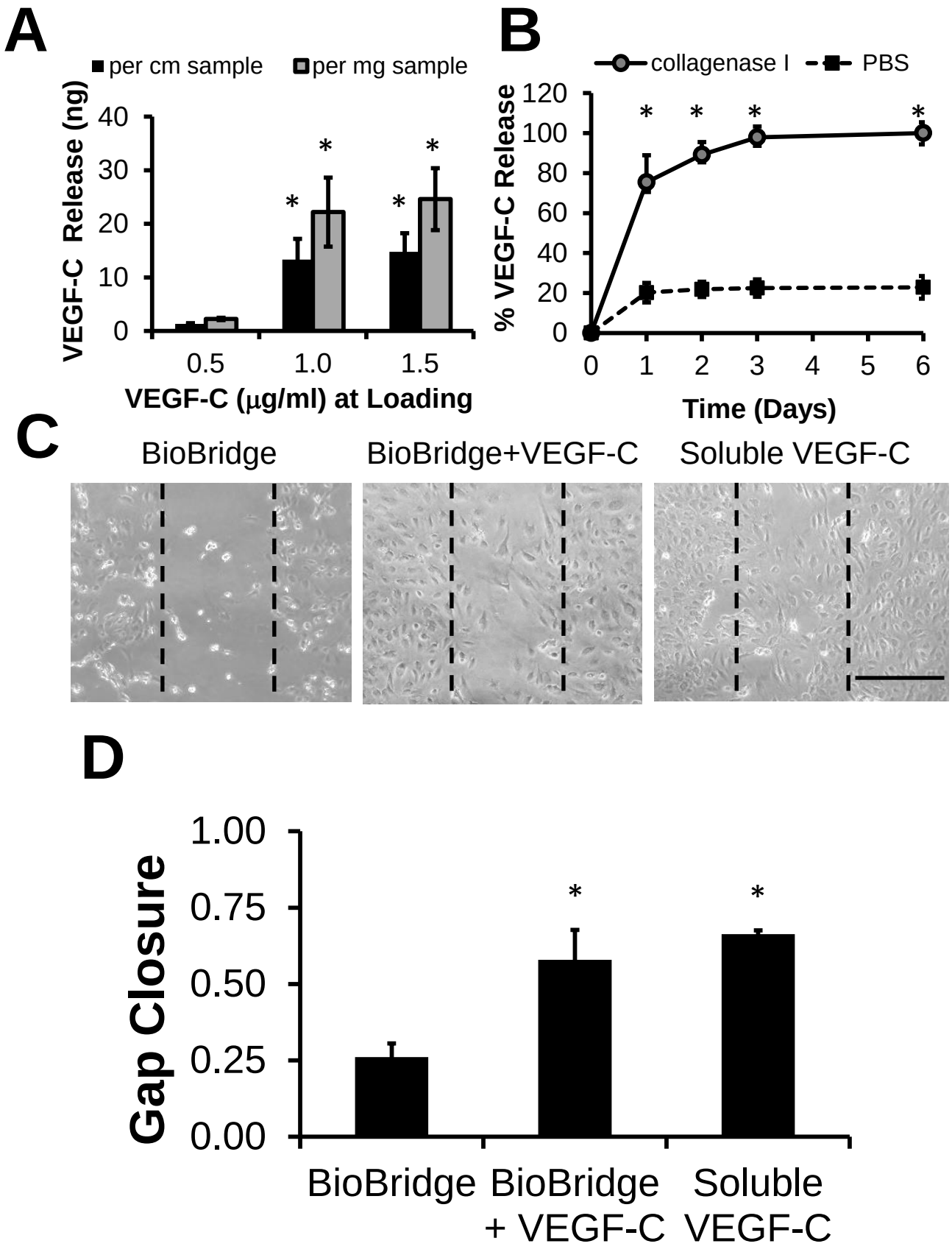
A
per cm sample
per mg sample
VEGF-C Release (ng)
40
30
20
10
0
0.5
1.0
1.5
VEGF-C (μg/ml) at Loading
B
collagenase I
PBS
% VEGF-C Release
120
100
80
60
40
20
0
0
1
2
3
4
5
6
Time (Days)
C
BioBridge
BioBridge+VEGF-C
Soluble VEGF-C
D
Gap Closure
1.00
0.75
0.50
0.25
0.00
BioBridge
BioBridge + VEGF-C
Soluble VEGF-C

Supplementary Fig. 6. VEGF-C release from scaffolds and quantification of the bioactivity of VEGF-C-conjugated scaffolds. A. Cumulative VEGF-C release from scaffolds after incubation in collagenase for 3 days for different VEGF-C concentrations used at the loading step. Data shown are normalized to cm scaffold and mg scaffold ($n \geq 3$); *significant comparison with 0.5 μg/ml loading condition . **B.** VEGF-C-conjugated scaffold samples were incubated in collagenase I or PBS for six days with medium collected and replaced at each time point. VEGF-C content in the collected samples was assayed by ELISA and plotted as percentage of total amount released in experiment per sample ($n \geq 3$). **C.** Human lymphatic endothelial cells (LECs) were cultured to confluence before a gap of defined size was made. Then, unsupplemented BioBridge collagen scaffolds (left panels), VEGF-C conjugated scaffolds (middle panels) or soluble VEGF-C (100 ng/ml) (right panels) were placed in the media. Dotted line indicates boundaries of the initial gap. **D.** Quantification of cellular migration expressed in percent of gap closure measured after 18 h culture. *$p < 0.05$ ($n \geq 3$). Scale bar= 300 μm.

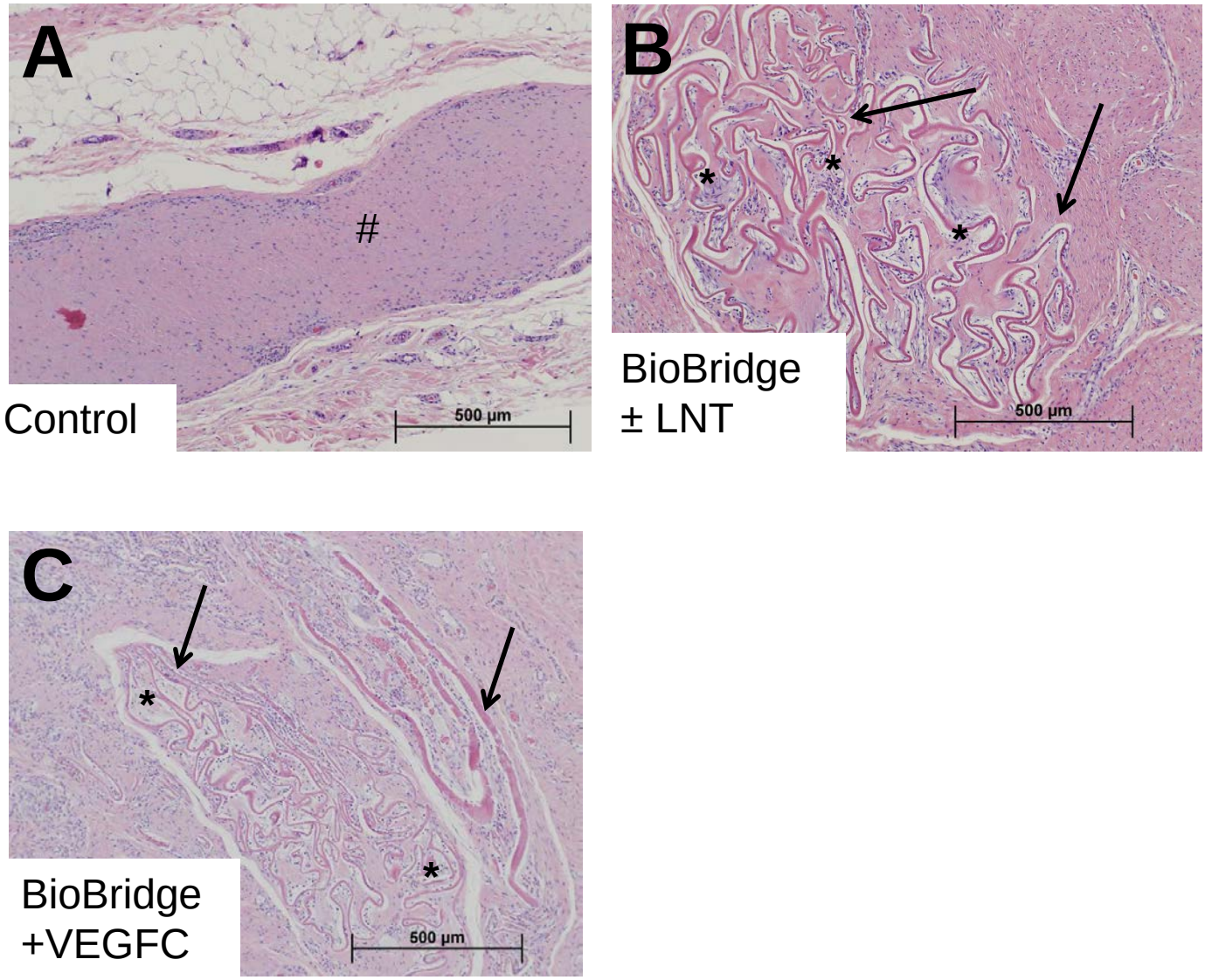

Supplementary Fig. 7. Histological analysis of the lymphedema sites with and without treatment. H&E staining of BioBridge scaffold 3 months post-transplantation (6-month study time point) for control (A), Biobridge ± LNT (B), and BioBridge + VEGFC (C) groups. Arrows show the folds of the scaffold integrated into the tissue, with cells infiltrating the inner space throughout the scaffold (denoted by *). The scar area is shown (#) in the control non-treated lymphedema site. Scale bar: 500 µm

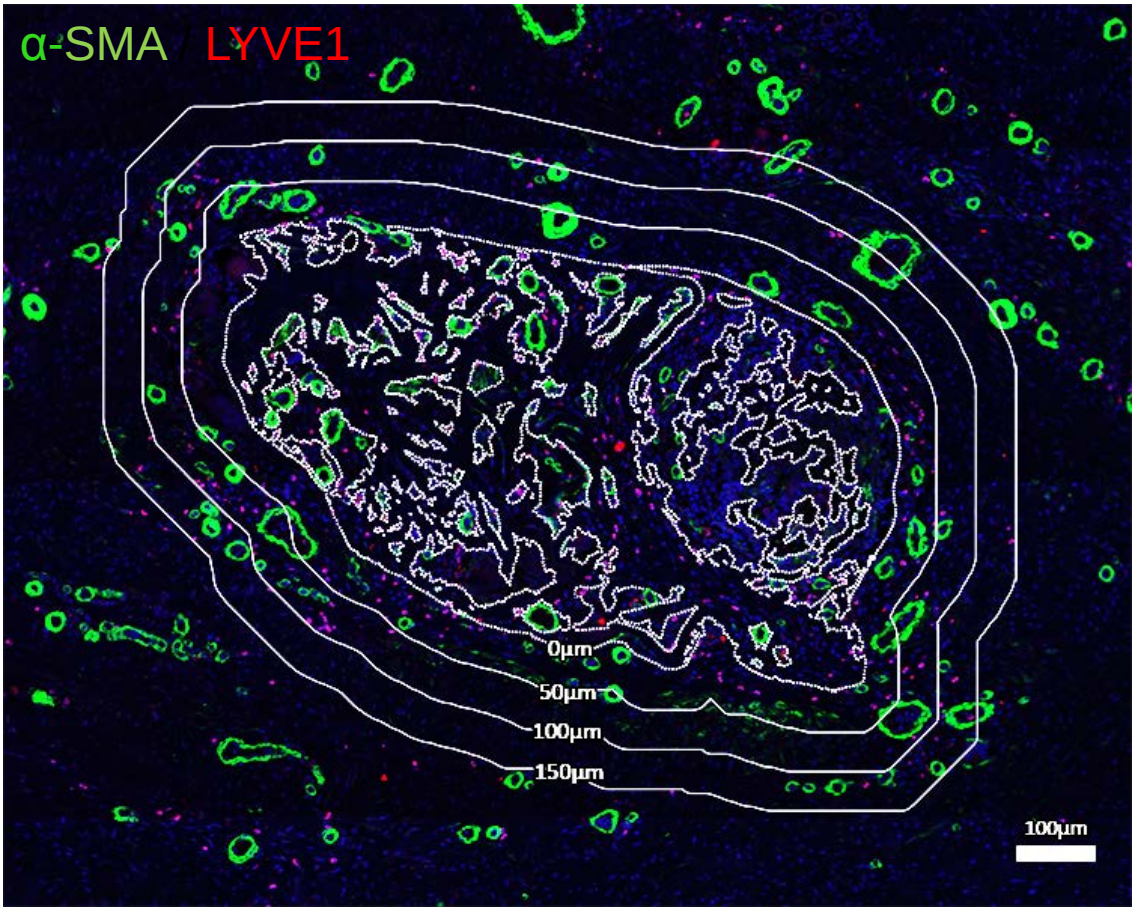

Supplementary Fig. 8. Quantification of lymphatic and vascular density in the periphery of the scaffold in subcutaneous tissue. The dotted white lines outline the scaffold pieces. A border (solid white line) was manually drawn around the periphery of the scaffold as the 0 μm radial distance from the scaffold. Then, rings that represent 50, 100, and 150 μm radial distances were automatically constructed using Image J software. Within each ring, the number of lymphatic collectors (α-SMA$^+$/LYVE1$^+$) and blood vessels (α-SMA$^+$/LYVE1$^-$) were counted and then expressed in the form of density (#/mm^2) by normalizing to the area of each ring. As an internal negative control for the regenerative effects of the scaffold, lymphatic and blood vascular densities were similarly quantified for tissue regions >2000 μm away from the scaffolds (not depicted in this image).

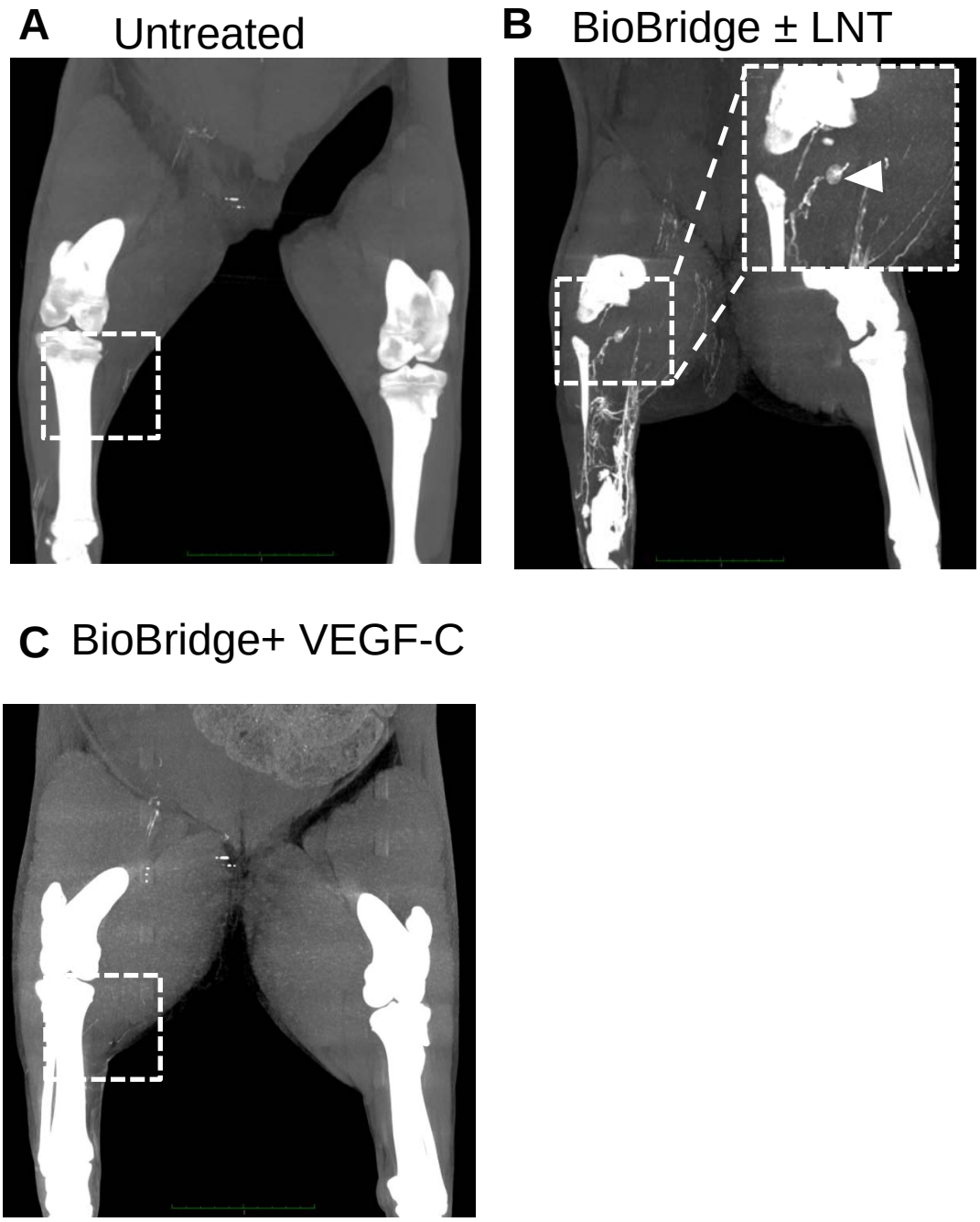

Supplementary Fig. 9. Representative contrast CT-scan imaging at three months after treatment. A. An untreated animal. B. An animal treated with BioBridge±LNT. C. An animal treated with VEGF-C conjugated collagen threads. The right limb had been injected with contrast dye prior to imaging. Box designates region of lymphatic regeneration. Note the vertical direction of the newly formed collectors in the groin of the animal treated with BioBridge±LNT.

Supplementary Table 1. Quantification of lymphatic collector ratio (lymphedematous/unoperated limb), expressed as a percentage at 0 and 3 months timepoints (n>3).

Treatment groups	0 months (before treatment)	3 months (after treatment)
BioBridge ± LNT	61%	76%
Untreated	45%	44%
BioBridge + VEGFC	76%	28%

Supplementary methods

MRI imaging of the hind limbs

At the study start point, negative control animals were subjected to MRI of the lymphatic vessels of the right limb (lymphedema) in order to visualize the anatomy of lymphatic structures and the presence of subcutaneous edema in the model. Here, animals were anesthetized with inhaled isoflurane 1-2% (MWI) only. A MRI of the pelvis and hind limbs was performed using a 3.0 Tesla MRI scanner (Signa 3T HDx, GE HealthCare, Pittsburgh, PA, USA) with an eight channel cardiac coil (3.0T HD Cardiac Array, GE HealthCare). A total of 3 ml of gadolinium contrast material (Magnevist, Bayer HealthCare, Leverkusen, NRW, Germany) was injected intradermally in the right hind paw. LAVA (3D spoiled gradient echo pulse sequence; TR 6.4ms, TE 3.1ms, flip angle 12, slice thickness 2.0 mm, matrix 512x512, field of view 48 cm) images were obtained at five minute intervals from the time of injection to 65 minutes post-injection**.**